Discovery of novel phosphatidylcholine-specific phospholipase C drug-like inhibitors as potential anticancer agents

Chatchakorn Eurtivong, Lisa I. Pilkington, Michelle van Rensburg, Reuben M. White, Harpreet Kaur Brar, Shaun Rees, Emily K. Paulin, Chris Sun Xu, Nabangshu Sharma, IvanhoeK.H. Leung, Euphemia Leung, David Barker, Jóhannes Reynisson

PII: S0223-5234(19)31071-2

DOI: https://doi.org/10.1016/j.ejmech.2019.111919

Reference: EJMECH 111919

To appear in: *European Journal of Medicinal Chemistry*

Received Date: 23 September 2019

Revised Date: 11 November 2019

Accepted Date: 26 November 2019

Please cite this article as: C. Eurtivong, L.I. Pilkington, M. van Rensburg, R.M. White, H.K. Brar, S. Rees, E.K. Paulin, C.S. Xu, N. Sharma, I.H. Leung, E. Leung, D. Barker, Jó. Reynisson, Discovery of novel phosphatidylcholine-specific phospholipase C drug-like inhibitors as potential anticancer agents, *European Journal of Medicinal Chemistry* (2019), doi: https://doi.org/10.1016/j.ejmech.2019.111919.

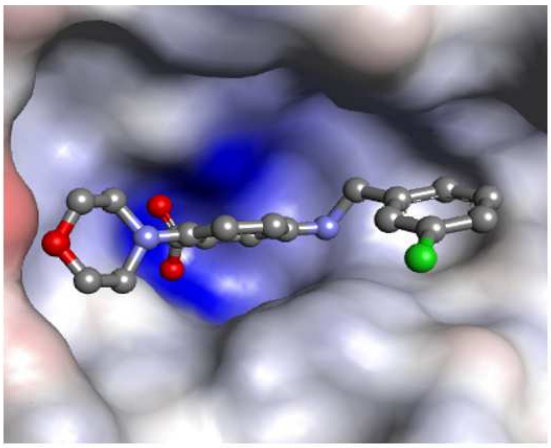

Inhibition of PC-PLC at IC_{50} 4.9 μM
Morpholinobenzoic acid

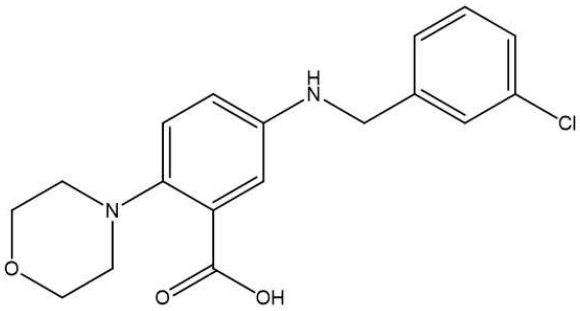

Discovery of Novel Phosphatidylcholine-Specific Phospholipase C Drug-like Inhibitors as Potential Anticancer Agents

*Chatchakorn Eurtivong,[1, 2] Lisa I. Pilkington,[1] Michelle van Rensburg,[1] Reuben M. White,[1] Harpreet Kaur Brar,[1] Shaun Rees,[1] Emily K. Paulin,[1] Chris Sun Xu,[3] Nabangshu Sharma,[1] Ivanhoe K. H. Leung,[1,4] Euphemia Leung,[3] David Barker[1] and Jóhannes Reynisson[*1,5]*

[1] School of Chemical Sciences, The University of Auckland, Private Bag 92019, Victoria Street West, Auckland 1142, New Zealand

[2] Chemical Science Program, Chulabhorn Graduate Institute, Chulabhorn Royal Academy of Science, Bangkok 10210, Thailand

[3] Auckland Cancer Society Research Centre, The University of Auckland, Private Bag 92019, Victoria Street West, Auckland 1142, New Zealand

[4] Maurice Wilkins Centre for Molecular Biodiscovery, The University of Auckland, Private Bag 92019, Victoria Street West, Auckland 1142, New Zealand

[5] School of Pharmacy and Bioengineering, Keele University, Hornbeam building, Staffordshire ST5 5BG, United Kingdom

*To whom correspondence should be addressed: School of Pharmacy and Bioengineering, Keele University, Hornbeam building, Staffordshire ST5 5BG, United Kingdom
E-mail: j.reynisson@keele.ac.uk, Tel. +44 (0)1782 733985

Abstract

Phosphatidylcholine–specific phospholipase C (PC-PLC) is a promising target for new anticancer treatment. Herein, we report our work in the discovery of novel drug-like PC-PLC inhibitors. Virtual screening led to the identification of promising hits from four different structural series that contain the molecular scaffold of benzenesulphonamides (**10**), pyrido[3,4-*b*]indoles (**22**), morpholinobenzoic acid (**84**) and benzamidobenzoic acid (**80**). 164 structural analogues were tested to investigate the chemical space around the hit series and to generate preliminary structurally activity relationships (SAR). Two of the pyrido[3,4-*b*]indoles (**22_10** and **22_15**) had comparable or better potency as D609, an established but *non-drug-like* PC-PLC inhibitor. Furthermore, three morpholinobenzoic acids (**84**, **84_4** and

84_5) had superior potency than D609. Therefore, this study paves the way towards the development of *drug-like* PL-PLC inhibitors as potential anticancer agents.

Keywords: virtual screening; similarity searching; molecular modelling; synthesis; pyrido[3,4-*b*]indoles; morpholinobenzoic acid; chemical space

1. Introduction

Phospholipase C (PLC) is a family of enzymes that mediate diverse cellular functions [1]. PLCs cleave phospholipids to generate by-products that play central roles in regulation of cellular processes: proliferation, differentiation, motility, apoptosis and gene expression [1-2]. A common by-product is diacylglycerol (DAG) that activates protein kinase C (PKC) to further phosphorylate downstream proteins and propagate an array of signalling events [1-2]. Unregulation of these signalling events can lead to the development of cancer. Thus, the homeostasis of the signalling pathways is crucially important to cellular health and to prevent the development of diseases such as cancer [1-2].

Phosphatidylcholine – specific phospholipase C (PC-PLC) is a PLC subtype that functions by preferentially cleaving phosphatidylcholine to generate DAG and phosphocholine as by-products. A wealth of evidence suggests that PC-PLC is involved in cancer development, including; increased expression in ovarian tumour cells [3] and highly metastatic triple-negative MDA-MB-231 breast cancer cell line [4], downregulation of HER2 oncogene upon PC-PLC inhibition [5], and linkages to hepatocarcinoma [6] and leukaemia progression [7]. Furthermore, it has been demonstrated that PC-PLC plays a crucial role in the development of atherosclerosis making PC-PLC and interesting target for the development of cardiovascular drugs [8].

A handful of PC-PLC inhibitors are known but are not considered to be *drug-like*. These are 2-aminohydroxamic acids [9], univalent anions [10], *N,N'*-dihydroxyureas [11], phospholipid

analogues [12] and the established xanthate, D609 (see molecular structures in Fig. 1) [13-14]. D609 is also known to modulate other biochemical targets such as the the K^+ channel, KCNQ1/KCNE1 [15] and sphingomyelin synthase [16]. Hence, it is desirable to identify novel inhibitors of PC-PLC with *drug-like* properties and with tractable synthetic routes for further development.

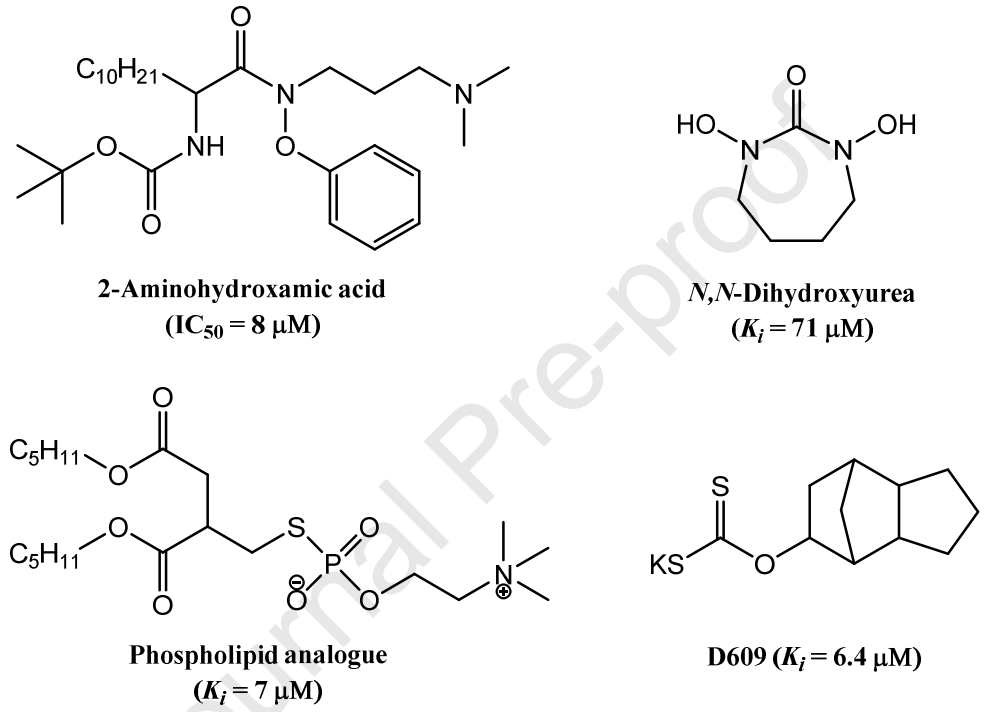

Fig. 1. Examples of known PC-PLC inhibitors and their reported inhibition activities. IC_{50} – the 50% inhibition concentration, K_i – dissociation constants.

The structure of eukaryotic PC-PLC is unknown and only prokaryotic PC-PLC enzymes have been structurally characterised. The most studied PC-PLC is isolated from *Bacillus cereus* [17]. In this paper, we describe a search for hit compounds against human PC-PLC for potential anticancer drug development using the virtual high throughput screening (vHTS) methodology, an effective method for identifying novel inhibitors for biomolecular targets [18-21]. The process relies on the structural similarity between PC-PLC$_{Bc}$ and mammalian PC-PLC, *i.e.*, the bacterial crystal structure was used as a model for its human counterpart.

This approach can be justified, as it was reported that PC-PLC$_{Bc}$ has antigenic similarity to mammalian PC-PLC [22] and can mimic similar responses to mammalian PLC, *e.g.*, enhancement of prostaglandin biosynthesis [23].

2. Results and Discussion

2.1. Pilot Virtual Screen

1×10^4 molecular entities were downloaded from the ChemBridge diversity collection [24]. These compounds were filtered based on Lipinski's rules [25], resulting in 8373 *drug-like* molecules. The docking scaffold used was the wild-type PC-PLC$_{Bc}$ crystal structure (structure shown in Fig. **2**) [17]. It can be seen that the catalytic site has three Zn^{2+} ions ligated to amino acids and water molecules. Zn1 is bridged to Zn3 by a water molecule and ligates to residues Asp55, His69, His118 and Asp122. Zn2 is ligated to two water molecules and amino acid residues His128, Glu146 and His142. Zn3 is ligated to amino acids Trp1, His14 and Asp122. Zn3 was selected as the centre of binding as it was reported that the Zn^{2+} ions play an important role for the catalytic cleavage by binding to charged phosphate groups on the phospholipid substrates [11,17,26].

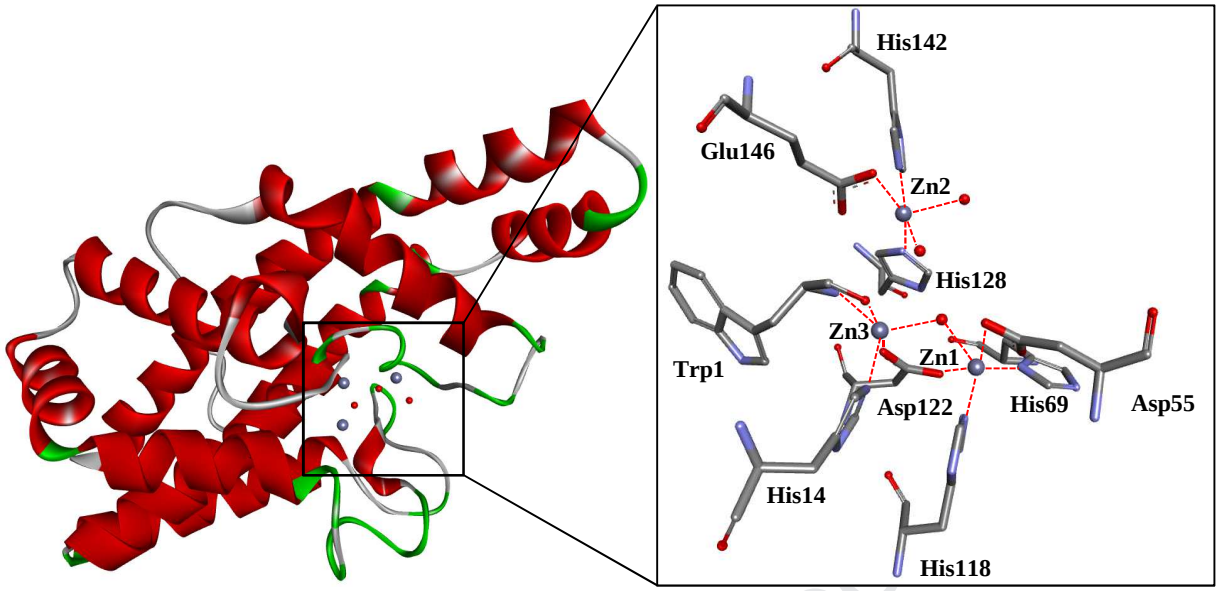

Fig. 2. The structure of wild-type PC-PLC$_{Bc}$ enzyme (PDB: 1AH7) [17]. The phospholipase monomer is displayed as red ribbons embedded with three catalytic Zn^{2+} ions and water molecules depicted as grey and red spheres respectively (left). Coordinating amino acids to the Zn^{2+} ions are represented as sticks and coloured by atom types (right).

Four scoring functions, GoldScore (GS) [27], ChemScore (CS) [28,29], Piecewise Linear Potential (ChemPLP) [30] and Astex Statistical Potential (ASP) [31] were implemented at 30% docking efficiency. Molecules without hydrogen bonding (HB = 0) and those that had scores GS < 55, CS < 26, ChemPLP < 65 and ASP < 25 were eliminated. The known D609 inhibitor (**33**) was docked to the catalytic site, and the output scores were used as criteria for the elimination process (endo-isomer: GS = 65.8, CS = 28.7, ChemPLP = 55.1, ASP = 55.1 and exo-isomer: GS = 76.9, CS = 30.0, ChemPLP = 58.8, ASP = 19.3). D609 (**33**) was used as a positive control throughout this study [13,14].

The initial elimination process resulted in 1721 molecules. These were re-docked at a higher efficiency (100%), *i.e.*, higher quality pose of the ligand was predicted. Molecules with HB = 0, GS < 60, CS < 34, ChemPLP < 65 and ASP < 28 were eliminated. Additionally, molecules with undesirable reactive, cytotoxic and chemically unstable moieties [32]. The remaining molecules were checked for the best predicted poses between the scoring functions and

whether a plausible binding mode was predicted, *e.g.*, unstrained poses, chemical groups directed towards Zn^{2+} ions to form electrostatic interactions and no lipophilic moieties facing the aqueous environment. In total, thirty-two compounds (see molecular structures **1-33** Fig. S1 in the Supplementary Information) were identified to be the most promising and were acquired from ChemBridge [24]. The compounds were tested with the PC-PLC Amplex Red assay (Molecular Probe, Inc.) that measures the activity of PC-PLC$_{Bc}$ and the results are shown in Fig. 3.

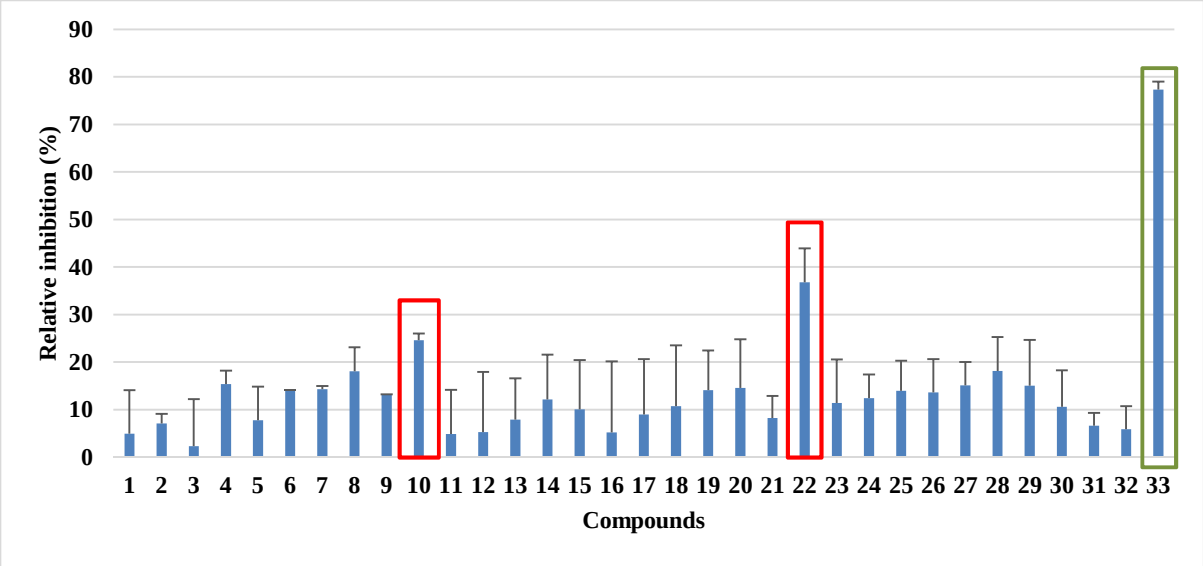

Fig. 3. Inhibition of PC-PLC$_{Bc}$ activity by the 32 virtual hits from the pilot screen at 10 μM single concentration using the Amplex Red biochemical assay. The standard deviations are shown. The positive control used is D609 (**33**) in green. Active hits were identified as having >15% inhibitory activity resulting in compounds **10** and **22** as bracketed in red.

The ligands were considered to be hits if they achieved levels of enzyme inhibition >15%, based on the fluorescence intensity emitted relative to the blank. Two hits were identified: 3-[(4-cyclohexylphenyl)sulfonamido]benzoic acid (**10**) and 1-[4-(trifluoromethyl)phenyl]-2,3,4,9-tetrahydro-1*H*-pyrido[3,4-*b*]indole-3-carboxylic acid (**22**) having 25% and 37% inhibition at 10 μM, the molecular structures are shown in Fig. 4. D609 (**33**), the accepted standard, gave inhibition close to 75%. Interestingly, both **10** and **22** have carboxylic acid

moieties that can potentially coordinate to the catalytic Zn^{2+} ions in the binding site suggesting that they '*activate*' the phosphate group on the phosphatidylcholine substrate instigating nucleophilic cleavage steps [26,33].

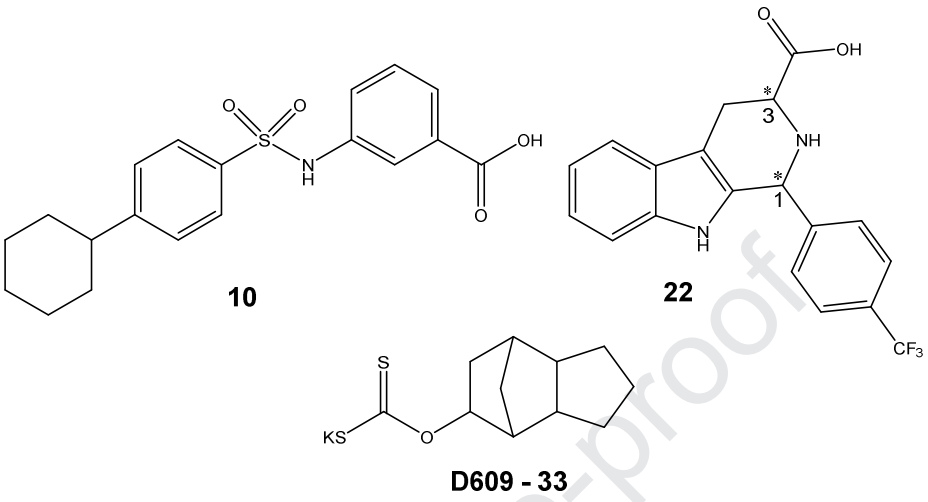

Fig. 4. The two hits **10** and **22** identified with the Amplex Red biochemical assay for activity against PC-PLC. The known inhibitor D609 (**33**) was used as a positive control [13,14]. The chiral centres (*) are shown in **22**.

In order to explore the structure activity relationship (SAR) of **10** and **22**, similar analogues were identified using eMolecules.com [34], a website that hosts commercially-available compounds. Similar ligands were found from ChemBridge [24], Chemical Diversity Inc (ChemDiv) [35] and InterBioScreen Ltd (IBS) [36]. The chemical series resulting from hits **10** and **22** were classified as the *N*-phenylbenzenesulphonamides and pyrido[3,4-*b*]indoles, respectively, based on their core scaffolds.

2.1.1. N-Phenylbenzenesulphonamides

Hit **10** demonstrated 25% inhibition in the biochemical assay and has a *N*-phenylbenzenesulphonamide core. A similarity coefficient of 0.7 was used to search for structurally similar compounds in eMolecules.com [34]. Twelve *N*-

phenylbenzenesulphonamides were purchased and tested; the molecular structures and results are given in Table S1 in the Supplementary Information. Only modest inhibitory activities against PC-PLC$_{Bc}$ was achieved by the members of this series and none of the derivatives was more potent than the original hit **10**. A detailed discussion on the SAR and molecular modelling are given in the Supplementary Information (Pages S7 –S9).

2.1.2. Pyrido[3,4-b]indoles

Hit compound **22** had a measured inhibition of 37%. It had a 2,3,4,9-tetrahydro-1*H*-pyrido[3,4-*b*]indole heterocyclic core with the pyridine moiety linked to a phenyl ring and a carboxylic acid with unknown stereochemistry at the two chiral centres, shown in Figure 4. A similarity coefficient value of 0.7 was used to search for structurally similar compounds using eMolecules.com [34]. Thirty-five indoles were purchased and their structures and inhibition data are given in Table S2 in the SI.

There is a clear indication of PC-PLC$_{Bc}$ inhibition for this series, with several derivatives showing improved potency over to the original hit (>37%) and even surpassing the established reference compound **33**. Generally, the best compounds have alkoxy and hydroxyl electron-donating groups at *meta* and *para* positions on the phenyl ring. 3,4-Dihydroxysubstitution on the phenyl rind (compound **22_10**) had the strongest inhibition effect (~75%), followed by 3,5-dimethoxy-4-hydroxy substitution (**22_14**) at ~60% and following closely by **22_12**, **22_15** (*p*-*N*,*N*-dimethyl), **22_11** and **22_13** ranging between 43 – 53% inhibition. Alkoxy substitutions alone showed modest inhibitory effects (**22_3**, **22_5**, **22_6**, and **22_8**). Single halogen substitutions did not improved efficacy with the exception of *m*-fluoro (**22_16**), whereas 2,4-dichloro (**22_20**) demonstrated improved inhibition (~44%). The remaining substituents on the phenyl ring include nitro (**22_26** and **22_25**) and

m-CF_3 (**22_23**), hydrogens (**22_ 1**) and alkyls (**22_28**, **22_27**, **22_29**, **22_30** and **22_32**), which did not improve potency. Replacing phenyl with pyridine (**22_34**) did not improve activity, whereas improved activity was seen with a naphthyl ring (**22_35**). Methyl (**22_33**) substantially reduced inhibition suggesting the importance of bulky aromatic systems. Introducing acetyl on the piperidine ring at R_5 (**22_31**) had detrimental effect on the potency.

Molecular modelling was conducted to understand the inhibition mechanisms of these ligands. Since they were tested as potential racemic mixtures, the diastereoisomer corresponding to the best activity was unclear. This problem was investigated by docking all four diastereoisomers (Table 1) using the most active compound **22_10**. The results revealed that the **(1*R*,3*S*)**-diastereoisomer scored best for the CS, ChemPLP and ASP functions. It also scored comparably well to the highest GS scoring **(1*S*,3*S*)-**diastereoisomer. It can therefore be argued that the (**1*R*,3*S***)-diastereoisomer is predicted to be the most active. Interestingly, visual inspection showed plausible binding modes (see. Fig. 5) for all four diastereoisomers, *e.g*., phenyl and indole moieties occupy lipophilic areas and the carboxylic acid moiety is facing the Zn^{2+} ions.

Table 1 Docking scores of the four possible diastereoisomers of the most active ligand **22_10**.

Compound	Compound	GS	CS	ChemPLP	ASP
PC_079 (SS)	**22_10 (1*S*,3*S*)**	75.6	45.0	84.3	43.8
PC_079 (RS)	**22_10 (1*S*,3*R*)**	69.5	44.1	83.5	41.5
PC_079 (RR)	**22_10 (1*R*,3*R*)**	64.1	43.0	77.6	42.4
PC_079 (SR)	**22_10 (1*R*,3*S*)**	73.8	46.4	95.3	45.5

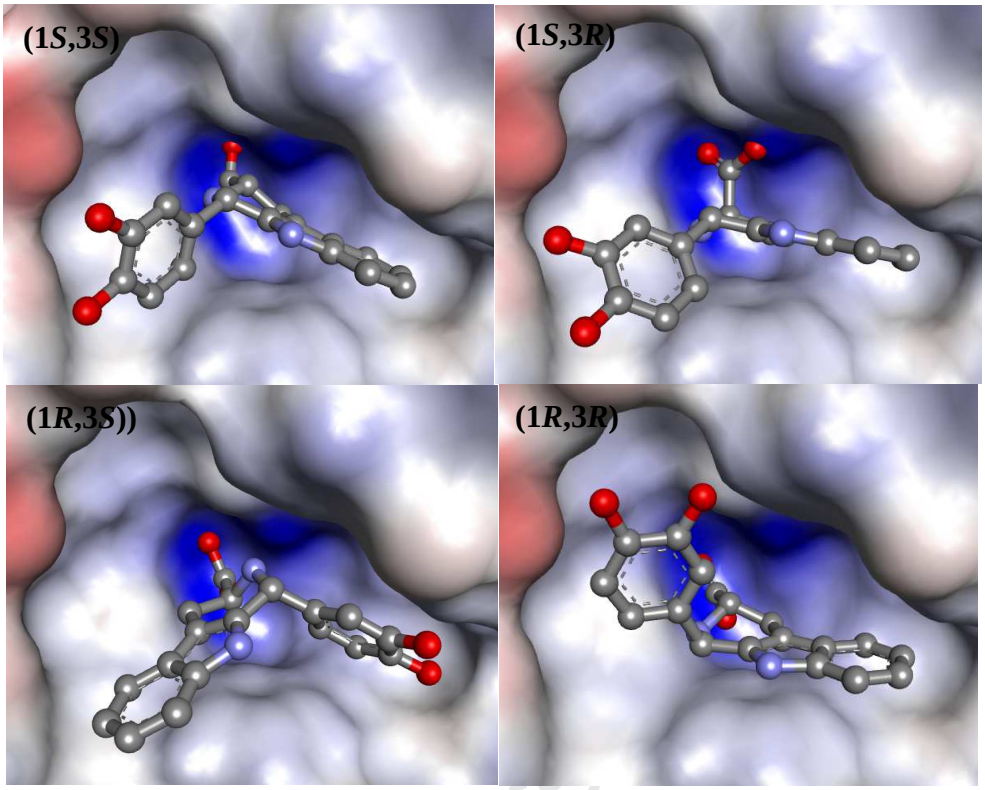

Fig. 5. The docked configurations of the four 1-(3,4-dihydroxyphenyl)-2,3,4,9-tetrahydro-1*H*-pyrido[3,4-*b*]indole-3-carboxylic acid (**22_10)** diastereomers in the PC-PLC$_{Bc}$ binding site. The protein surface is rendered. Red and blue surfaces depicts negative and positive partial charge respectively whereas grey shows neutral lipophilic areas. The hydrogens are removed for the ligands for clarity.

All 1-phenyl-(**1*R*,3*S***)-2,3,4,9-tetrahydro-1*H*-pyrido[3,4-*b*]indoles **22_1** to **22_32**, despite different substitution patterns on the phenyl ring, show high similarity in binding modes and scores. The general binding mode and interactions are represented by **22_10** in Fig. 6. The phenyl group is situated close to lipophilic areas partly consisting of Phe66 and Phe70 residues where they are expected to form π–π stacking, whereas the tricyclic 2,3,4,9-tetrahydro-1*H*-pyrido[3,4-*b*]indole heterocycle occupies a lipophilic region formed by residues Ala3, Tyr56 and Phe66. Hydrogen bonding was predicted with His69 *via* the carboxylic acid. In some cases, Glu146 formed hydrogen bond with pyridine, *e.g.*, ligand **22_15**. The carboxylic acid functional group facing the deeply buried positively charged regions are expected to form coordination bonds with the Zn^{2+} ions.

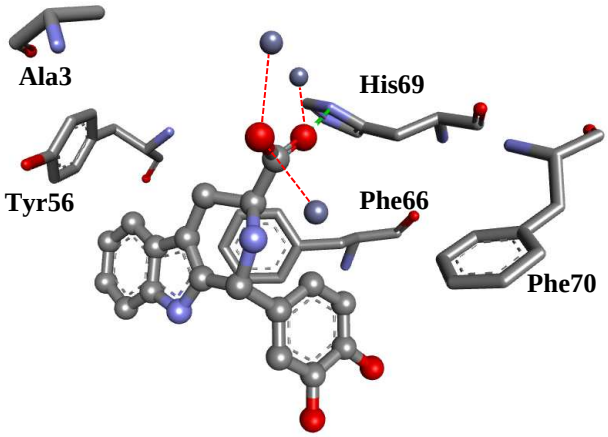

Figure 6. Binding interactions of **(1*R*,3*S*)-22_10** in the PC-PLC$_{Bc}$ binding site has hydrogen bonding with His69 residue depicted as a green dotted line. Zn^{2+} ions are depicted as unconnected grey spheres and are coordinated by the carboxylic acid functionality shown as red dotted lines. Hydrophobic amino acid residues Ala3, Tyr56, Phe66 and Phe70 are shown. The hydrogens are removed for the ligand and amino acid residues for clarity.

In order to extend the SAR of the indoles further, thirty-six derivatives were synthesised. A detailed description of the synthesis, synthetic procedures, characterisation of compounds is given in the Supplementary Information (Pages S12 – S34). The stereochemistry of these ligands was controlled for the carbon 3 site to better understand its effect. The derivatives were therefore tested as isomeric mixtures of *cis*/*trans* isomers. Three main types of ligands were made; carboxylic acids, their esters and planar aromatic derivatives with both chiral centres removed. The phenyl ring was decorated with methoxyl and hydroxyl substituents. The molecular structures and their activity against PC-PLC are given in Tables S9 – S11 in the SI.

Unfortunately, only three of the synthesised derivatives had good potency, two carboxyl acid derivatives and one ester. The aromatisation of the piperidine moiety to pyridine rendered the derivatives marginally active or simply inactive. The acids **(3*S*)-22_S5** and **(3*R*)-22_S8** do not have the same stereochemistry but both are active, supporting the modelling of **22_10**, *i.e.*, all four stereoisomers can fit into the binding pocket. The ester derivative **(3*S*)-22_S15**

has the same substitution pattern on the phenyl ring as **(3*S*)-22_S5**, *m*-OCH_3 and *p*-OH. A detailed discussion of the SAR is given in the SI pages S37 and S38.

Interestingly, tadalafil (see Fig. S3 in the SI), a marketed drug, consists of the 2,3,4,9-tetrahydro-1*H*-pyrido[3,4-*b*]indole core as its molecular scaffold. Tadalafil is a phosphodiesterase type 5 (PDE5) inhibitor and is orally available as a treatment for erectile dysfunction [37]. This suggests the 2,3,4,9-tetrahydro-1*H*-pyrido[3,4-*b*]indole core is likely to be compatible for use in the clinic with acceptable pharmacokinetic profile.

2.2 Main Screen

The success of the pilot screen encouraged further search of more inhibitors using the same methodology. The rest of the ChemBridge´s Diversity collection, 4×10^4 molecular entities, were filtered using Lipinski's Rule of Five, leaving ~3.3×10^4 *drug-like* molecules. All four scoring functions available in the GOLD software suite were used: GS, CS, ChemPLP and ASP. The consensus concept used in the pilot screen was applied, *i.e.*, only ligands that scored well with all scoring functions and have predicted hydrogen bonding were taken forward [38, 39]. The first filter criteria was: GS > 55, CS > 25, ChemPLP > 65, ASP > 25 and HB $\geq$ 1. This resulted in 5249 candidates, which were re-docked at 100% search efficiency. The candidates were filtered through a second score criteria: GS > 55, CS > 25, ChemPLP > 70 and ASP > 25. Furthermore, compounds with good hydrogen bonding activities were selected (HB $\geq$ 1) resulting in 871 candidates. Subsequently, ligands with carboxylic acid functionality and moieties that ionise to form negative charges were taken forward. This approach assumed the best inhibitors had the ability to coordinate to the Zn^{2+} ions. One hundred and fifty-five candidates were selected that had the carboxylic and sulphonic acid moieties. Candidates with undesirable reactive, cytotoxic and chemically

unstable moieties [32]. All the ligands were visually inspected for plausible binding modes and similar binding pose between the four scoring functions, *i.e.*, good overlays between the predicted binding poses. In total, fifty-four compounds **34**-**87** were purchased for testing and they are shown in Fig. S4 in the SI.

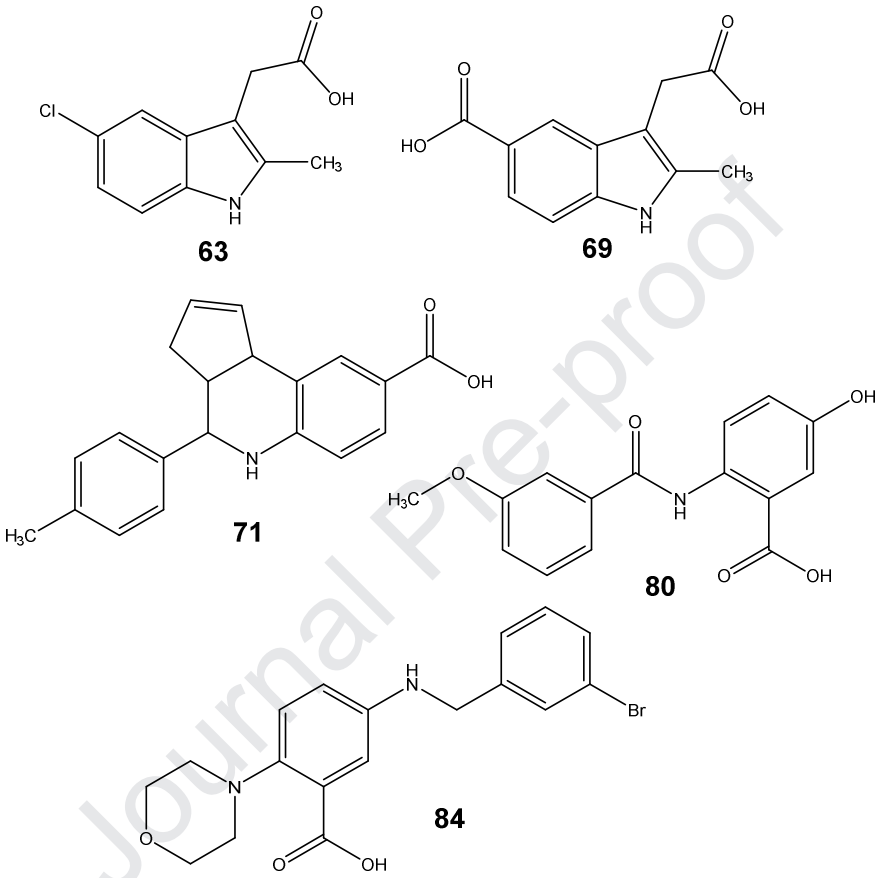

Fig. 8. The molecular structures of the hits **63** (65%), **69** (60%), **71** (54%), **80** (47%) and **84** (80%) tested with the Amplex Red biochemical assay for PC-PLC inhibition at 10 µM.

Four compounds emerged as strong hits with inhibition >50% using the Amplex Red biochemical assay (see Fig. 8). Hit **84** showed the best potency (80%) followed by **63** (65%), **69** (60%) and **71** (54%). Hits with medium inhibitory activities (25 – 50%) were also seen **37** (25%), **48** (43%), **49** (28%), **73** (40%), **74** (29%) and **80** (47%). Interestingly, multiple compounds of the same family appeared as actives from the main screen: indole-3-acetic

acids (**63** and **69**) and benzamidobenzoic acids (**48**, **74** and **80**). Four more benzamidobenzoic acid derivatives were also found to exhibit weak activities (<25%): **55**, **62**, **72** and **78**.

Similarity searches were conducted based on the molecular scaffolds of **71** and **84**, as well as the more modest benzamidobenzoic acid ligand **80**. The search results revealed no similar compounds to **71** at the 0.7 threshold limit. Forty-three derivatives of **84** and twenty derivatives of **80** were obtained using the search coefficient value of 0.7. Although the indole-3-acetic acids **63** and **69** displayed strong potency, they were omitted from the search as potential false positives. The compounds resemble the plant growth hormone, auxin (see molecular structure in Fig. **S5** in the SI). Naturally, auxin is biosynthesised from its amino acid precursor, tryptophan [40], and is reported to possess anticancer activities in the presence of horseradish peroxidase [41-43]. The mechanism proposed was generation of free radicals that resulted in apoptosis [41-43]. Auxin alone did not induce cytotoxicity in human melanoma cells [44], which confirmed their inactivity *in vitro*.

2.2.1. 2-Morpholinobenzoic acids

Hit **84** emerged as the strongest inhibitor from the main screen with the impressive 80% inhibition (at 10 μM). Compound **84** has a 2-morpholinobenzoic acid scaffold linked to a benzyl group by an amine, with the amine positioned *para* to the morpholine ring. Forty-one analogues of **84**, classified as the 2-morpholinobenzoic acids, were purchased for testing; the molecular structures are shown in Table S12 in the SI as well as the assay results. Compounds **84_1** to **84_33** have various substitution groups around the phenyl ring. Compounds **84_34** to **39** have various heterocyclic and aromatic groups linked to the 5-amino functionality. The 5-amino group is replaced with a hydrogen for **84_40**. Compound **84_41** contains a piperazine ring instead of a morpholine.

Generally, various substitution patterns around the phenyl ring, did not impact on the inhibitory effects of the compound with levels mainly ranging between 65 – 75% for compounds **84_1** to **84_33**. Unsubstituted phenyl (**84_1**) had 67% potency against the PC-PLC enzyme. Most single halogen substitutions (**84** and **84_2** to **7**) had inhibition >70% with *o*- (**84_4**) and *m*-chloro (**84_5**) excellent inhibition at 89%, whereas dual *o*- and *p*-chloro substitution (**84_8**) had reduced activity at 65%. Introducing *o*-CF_3 (**84_9**), *p*-SCH_3 (**84_10**), single alkoxys (**84_11** to **16**), double alkoxys (**84_17** to **24**), halogen and alkoxy combinations (**84_25** to **29**), single alkyls (**84_30** to **32**) and 1-pyrrolidine (**84_33**) resulted in inactivity.

Compounds **84_34** to **39** showed activity in the absence of benzyl groups at the R_1 site and with inhibition > 68%. A notable exception was the 2-phenylacetamide functional group, which displayed significant loss in activity suggesting detrimental effects of amides to the SAR. The absence of 5-amino group (**84_40**) and replacement of morpholine for 4-methylpiperazine-1-yl (**84_41**) also resulted in significant loss in potency.

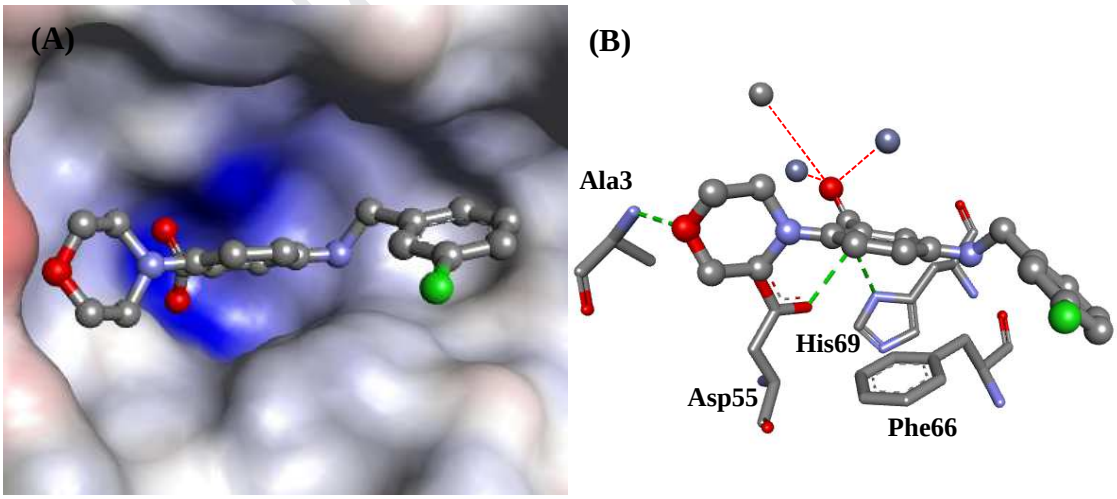

Fig. 9. The docked configuration of 2-morpholinobenzoic acid **84_5 (A)** in the PC-PLC_{Bc} binding site. The protein surface is rendered. Red and blue surfaces depicts negative and positive partial charge whereas grey shows neutral lipophilic areas. **(B)** Binding interactions with **84_5** show Zn^{2+} ions as grey unconnected spheres form coordinate bonds depicted as red dotted lines, whereas hydrogen bonding are depicted as green dotted lines with residues Ala3 and Asp55.

Modelling of the 2-morpholinobenzoic acid **84_5** (see Figure 9 A and B) showed the phenyl group occupying a lipophilic space surrounded side chains of Phe70, Tyr79 and Thr133. The benzoic acid core is seen directly above a hydrophobic basin formed by Phe66 that could form π–π stacking stabilising the enzyme-inhibitor complex. Furthermore, the morpholine to Ala3 hydrogen bond interaction can be rationalised as a selective interaction. The reason that piperazine analogue (**84_42**) demonstrated significant reduction in activity is most likely due to it having no hydrogen bond with Ala3.

2.2.2. Benzamidobenzoic acids

Benzamidobenzoic acids **48**, **74** and **80** were identified from the main screen with relative inhibition 25 – 50%, whereas **55**, **62**, **72** and **78** showed were weaker inhibitors (<25%). From this series, hit **80** showed the strongest inhibition (47%) featuring a 3-methoxyphenyl moiety linked to benzoic acid by an amide functionality. Hits **48** and **74** had non-aromatic ethylcyclohexanes and benzyl moieties as replacements of the phenyl ring. Hit **55** replaces phenyl with tolylsuphane, and hits **62**, **72** and **78** replaced phenyl with benzyl moieties.

Twenty structurally similar derivatives were identified from a similarity search based on the molecular scaffold of **80** and were acquired for testing, the results and structures are given in Table S13 in the SI. Unfortunately, this series had weak activity and no improved ligands were found. Detailed discussion of the SAR and modelling of **80** is given in the SI (pages S48 – S49).

2.3. Inhibition and binding studies

The pilot and main screens resulted in the 1*H*-pyrido[3,4-*b*]indoles **22** and 2-morpholinobenzoic acids **84** as the most promising series for inhibition of PC-PLC activity. The best ligands were chosen for dose response measurements: two compounds, **22_10** and **15**, from the 1*H*-pyrido[3,4-*b*]indoles and three compounds, **84** and derivatives **84_4** and, **84_5**, from the 2-morpholinobenzoic acid series. The derived IC_{50} values (50% inhibition concentration) are shown in Table 2. In addition, the binding constant values (K_D) for **84** and derivative **84_4** against recombinant PC-PLC$_{Bc}$ were also measured (Supplementary Figures S7–S9). Interestingly, only **22_15** displayed weaker activity than D609, whereas the most active 2,3,4,9-tetrahydro-1*H*-pyrido[3,4-*b*]indole derivative, **22_10**, showed comparable potencies to the 2-morpholinobenzoic acids **84**. The binding constants of **84** and **84_4** are similar to **33**, in agreement with the measured IC_{50} values.

Table 2. Inhibition concentration at 50% (IC_{50}) and binding constant (K_D) values of the 2,3,4,9-tetrahydro-1*H*-pyrido[3,4-*b*]indole and 2-morpholinobenzoic acid derivatives against PC-PLC. The IC_{50} values are the averages of five replicates using the Amplex Red biochemical assay. Six different concentrations were used to derive the IC_{50} values: 0, 0.1, 0.4, 1.1, 3.3 and 10.0 μM. The K_D values are the averages of three replicates using the intrinsic fluorescence assay. * The K_D value for **84_5** was not determined due to spectral overlap in fluorescence emission. Compound **33** (D609) is the positive control. $KDI_{2a/2b}$ (Known Drug Index) values reflecting the drug-likens of the ligands. KDI_{2a} has theoretical maximum of 6.0 and KDI_{2b} of 1.0, the higher values the more *drug-like*.

Compound	**IC_{50} (μM)**	**K_D(μM)**	**$KDI_{2a/2b}$**
33 (D609)	8.08 ± 0.65	216 ± 8.0	4.66 / 0.19
22_10	3.10 ± 0.03	-	5.06 / 0.29
22_15	10.86 ± 0.56	-	5.71 / 0.74
84	3.69 ± 0.23	342 ± 3.9	5.94 / 0.94
84_4	3.60 ± 0.19	325 ± 3.0	5.94 / 0.94
84_5	4.90 ± 0.21	n.d.*	5.94 / 0.94

It can be stated that two hit series have been established for further development against PC-PLC, both displaying enhanced potency as compared to the standard D609 (**33**) ligand.

2.5. Chemical Space

The calculated molecular descriptors; molecular weight (MW), rotatable bonds (RB), hydrogen bond donors and acceptors (HD/HA), octanol / water partition coefficient (log P) and polar surface area (PSA) for all the compounds are within the boundaries of *drug-like* chemical space, *i.e.*, compounds satisfied Lipinski's filters [25], and Veber's rules [45]. The molecular descriptors and the results of the scoring functions are given in Tables S14 – S16 in the SI.

Furthermore, the *drug-like* qualities of the compounds were derived for the hit compounds by calculating the *Known Drug Index* (KDI) and the results are shown in (see Table 2) [46]. The KDI reflect the overall balance of the molecular properties calculated based on statistical distribution of Known Drug Space for the six molecular descriptors used. KDI_{2a} is additive with a theoretical maximum of 6.0 and for KDI_{2b} the indexes for each descriptor are multiplied giving 1.0 as its maximum. The average for KDI_{2a} for known drugs is 4.08 (±1.27) and all of the new hit compounds have values > 5 except for D609 (33). The same trend is seen of the KDI_{2b}, the hit compounds have much higher values than D609 with the **84** series all having 0.94, and with the average of know drugs being 0.18 (±0.20), very well balanced physicochemical properties for biological systems.

3. Conclusion

A virtual screen was conducted against PC-PLC, a promising anticancer target. 5×10^5 molecular entities of the ChemBridge Diversity library were screened and 86 of those were

tested using the Amplex Red biochemical assay at a single concentration (10 µM). Four potent hits with the molecular scaffolds of benzenesulphonamides, pyrido[3,4-*b*]indoles, morpholinobenzoic acids and benzamidobenzoic acids were identified. In order to establish a SAR 164 structural analogues were tested. The inhibition at 50% values (IC_{50}) were derived for the five most active compounds. The morpholinobenzoic acids **84, 84_4** and **84_5** had IC_{50} values of 3 - 5 µM with the pyrido[3, 4-*b*]indole **22_10** at similar potency, 3.10 µM. For comparison, the established inhibitor **33** (D609) was measured to have an IC_{50} value of 8.08 µM. The Known Drug Indexes (KDI), which gauge the drug-likeness of ligands, gave very favourable results, far surpassing the established D609 ligand. This means that two novel *drug-like* inhibitor classes were identified for PC-PLC enabling a drug discovery programme to be developed for this bio-molecular target.

4. Materials and Methods

4.1. Modelling

The crystal structure was obtained from Protein Data Bank (PDB) [47] ID: 1AH7[17] with resolution 1.50 Å. The Scigress v2.6 program [48] was used to prepare the crystal structure for docking, *i.e.*, hydrogen atoms were added and crystallographic water molecules removed. The centre of PC-PLC$_{Bc}$ binding pocket was defined as the position of Zn^{2+} ion (x = 42.4820, y = 22.996, z = 8.556) with 10 Å radius. The basic amino acids lysine and arginine were defined as protonated. Furthermore, aspartic and glutamic acids were assumed to be deprotonated. The GoldScore (GS)[27], ChemScore (CS)[28][29], Piecewise Linear Potential (ChemPLP)[30] and Astex Statistical Potential (ASP)[31] scoring functions were implemented to validate the predicted binding modes and relative energies of the ligands using the Genetic Optimisation for Ligand Docking software package (GOLD) version 5.4. This screening protocol used has been successfully applied to identify inhibitors for different

molecular targets such as phospholypase C- γ [49], autophagy complexation Atg5-Atg16 [50], tyrosyl-DNA phosphodiesterase 1 [51] and heat shock protein 90 [52]. The virtual high throughput screen was conducted with the ChemBridge diversity collection of 5×10^4 entities. Substructure and Tanimoto similarity methods [53] were used to identify structurally similar compounds through commercially available databases (see results and discussion). The Dragon version 7.0 [54] software was used to calculate for six mainstream molecular descriptors; molecular weight (MW), octanol-water partition coefficient P (Log P), rotatable bonds (RB), hydrogen bond donors (HD) and acceptors (HA) and polar surface area (PSA).

4.2. In vitro PC-PLC activity assays

Relative changes of PC-PLC activities were determined using the Amplex Red assay kit (Molecular Probe, Inc.), as described by the manufacturer. Briefly, PC-PLC activity was determined by adding the 0.01U PC-PLC protein to a reaction mixture containing 0.4 mM Amplex Red, 1 unit/mL horseradish peroxidase, 4 unit/mL alkaline phosphatase, 0.1 unit/mL choline oxidase, and 0.5 mM phosphotidylcholine (PtdCho) in 1X Reaction Buffer (50 mM Tris-HCl, pH 7.4, 0.14 M NaCl, 10 mM dimethylglutarate, 2 mM $CaCl_2$). Phosphocholine released from PtdCho by PC-PLC was converted to choline by alkaline phosphatase, which choline was oxidized to form H_2O_2. In the presence of horseradish peroxidase, the H_2O_2 reacts with Amplex Red to generate the fluorescent product, resorufin, which was detected using λ_{ex} = 560 nm and λ_{em} = 590 nm on the EnSpire multimode plate reader.

4.3. Recombinant PC-PLC$_{Bc}$ production

Plasmid encoding the full length PC-PLC$_{Bc}$ was obtained from Dr Ries Langley of Faculty of Medical and Health Sciences, The University of Auckland. The vector was a modified pET-21a(+) that enables the production of recombinant proteins with an N-terminal His6 tag and a

3C Protease cleavage site. The plasmid was transformed into *Escherichia coli* BL21(DE3) competent cells in the presence of 50 µg/mL ampicillin. Expression of PC-PLC$_{Bc}$ was induced using 0.5mM isopropyl 1-thio-β-D-galactopyranoside (IPTG) at 18°C for 16 hours. The harvested cells were resuspended in lysis buffer (50 mM Tris pH 8.0, 150 mM NaCl, 5 mM imidazole, 0.1 mM $ZnSO_4$, 5% glycerol) and then lysed by sonication. The protein was purified using a HisTrap HP column (GE Healthcare) charged with Ni^{2+} ions, connected to an ÄKTA START protein purifier system (GE Healthcare). The polyhistidine-tagged PC-PLC$_{Bc}$ was eluted using elution buffer (250 mM imidazole, 50 mM Tris-HCl pH 8.0, 150 mM NaCl, 5% glycerol, 0.1 mM $ZnSO_4$). The polyhistidine tag was then removed by incubation with GST-3C protease (PreScission Protease) in the presence of 2 mM dithiothreitol (DTT) at 4°C for 12 hours. This was followed by reverse purification using a His-Trap HP column to remove the cleaved polyhistidine tag. The recombinant PC-PLC$_{Bc}$ produced had a 14-amino acid pro-peptide extension at its N-terminal, which was cleaved by incubation with trypsin (sequencing grade modified Trypsin, Promega) using a 1:100 protease to protein ratio, at 37°C for 20 min at 90 rpm to obtain the fully functional protein [55, 56]. The trypsin was deactivated by heating at 50 °C and the protein was further purified by size exclusion chromatography using a HiPrep 16/60 Sephacryl S-100HR gel filtration column.

4.4. Binding constant measurement by intrinsic tryptophan fluorescence

Assay contained 5 µM of PC-PLC$_{Bc}$ and varying concentrations of compounds in 1 mM 3,3-dimethylglutaratic acid (pH 7.5) and 0.1 mM $ZnSO_4$ (90 µL volume). All experiments were conducted by using 96-blackwell microplates (Eppendorf). Fluorescence were measured by using a multimode plate reader (Perkin Elmer). Excitation wavelength was 280 nm and the fluorescence emission spectra were measured between 300-450 nm. K_D was obtained by

using the following equation for non-linear curve fitting using SigmaPlot 14.0 (Systat Software, USA).

$$\Delta_{obs} = \frac{\Delta_{max} \times [L_T]}{K_D + [L_T]}$$

In which $[L_T]$ denotes the total ligand concentration, Δ_{obs} denotes changes in fluorescence intensity and Δ_{max} as the maximum change in fluorescence intensity.

Acknowledgements

We are very grateful for the financial support from the Cancer Society of New Zealand (Ref: 17.01) and the Breast Cancer Partnership, Health Research Council, New Zealand (Ref: 17/671).

References

[1] C.M. Vines, Phospholipase C, Adv. Exp. Med. Biol. 740 (2012) 235-254.

[2] J.B. Park, C.S. Lee, J.H. Jang, J. Ghim, Y.J. Kim, S. You, D. Hwang, P.G. Suh, S.H. Ryu, Phospholipase signalling networks in cancer, Nat. Rev. Cancer 12 (2012) 782-792.

[3] F. Spadaro, C. Ramoni, D. Mezzanzanica, S. Miotti, P. Alberti, S. Cecchetti, E. Iorio, V. Dolo, S. Canevari, F. Podo, Phosphatidylcholine-Specific Phospholipase C Activation in Epithelial Ovarian Cancer Cells, Cancer Research. 68 (2008) 6541-6549.

[4] L. Abalsamo, F. Spadaro, G. Bozzuto, L. Paris, S. Cecchetti, L. Lugini, E. Iorio, A. Molinari, C. Ramoni, F. Podo, Inhibition of phosphatidylcholine-specific phospholipase C results in loss of mesenchymal traits in metastatic breast cancer cells, Breast Cancer Res. 14 (2012) R50.

[5] L. Paris, S. Cecchetti, F. Spadaro, L. Abalsamo, L. Lugini, M.E. Pisanu, E. Iorio, P.G. Natali, C. Ramoni, F. Podo, Inhibition of phosphatidylcholine-specific phospholipase C downregulates HER2 overexpression on plasma membrane of breast cancer cells, Breast cancer research : BCR. 12 (2010) R27.

[6] W. Xingzhong, H. Lu, L. Zhou, Y. Huang, H. Chen, Changes of Phosphatidylcholine-Specific Phospholipase C in Hepatocarcinogenesis and in the Proliferation and Differentiation of Rat Liver Cancer Cells. Cell Bio. Int. 21 (1997) 375-381.

[7] I. Plo, D. Lautier, T. Levade, H. Sekouri, J.P. Jaffrézou, G. Laurent, A. Bettaïeb, Phosphatidylcholine-specific phospholipase C and phospholipase D are respectively implicated in mitogen-activated protein kinase and nuclear factor kappaB activation in tumour-necrosis-factor-alpha-treated immature acute-myeloid-leukaemia cells, Biochem. J. 351 (2000) 459-467.

[8] H.Y. Li, L. Zhang, D.L. Yin, Y. Zhang, J. Y. Miao, Targeting Phosphatidylcholine-Specific Phospholipase C for Atherogenesis Therapy, Trends Cardiovas. Med. 20 (2010) 172-176.

[9] P. González-Bulnes, A. González-Roura, D. Canals, A. Delgado, J. Casas, A. Llebaria, 2-Aminohydroxamic acid derivatives as inhibitors of Bacillus cereus phosphatidylcholine preferred phospholipase C PC-PLCBc, Bioorg. Med. Chem. 18 (2010) 8549-8555.

[10] S.E. Aakre, C. Little, Inhibition of Bacillus cereus phospholipase C by univalent anions, Biochem. J. 203 (1982) 799-801.

[11] S.F. Martin, B.C. Follows, P.J. Hergenrother, C.L. Franklin, A novel class of zinc-binding inhibitors for the phosphatidylcholine-preferring phospholipase C from Bacillus cereus, J. Org. Chem. 65 (2000) 4509-4514.

[12] S.F. Martin, Y. Wong, A.S. Wagman, Design, Synthesis, and Evaluation of Phospholipid Analogs as Inhibitors of the Bacterial Phospholipase C from Bacillus cereus, J. Org. Chem. 59 (1994) 4821-4831.

[13] R. Adibhatla, J. Hatcher, A. Gusain, Tricyclodecan-9-yl-Xanthogenate (D609) Mechanism of Actions: A Mini-Review of Literature, Neurochem. Res. 37 (2012) 671-679.

[14] E. Amtmann, The antiviral, antitumoural xanthate D609 is a competitive inhibitor of phosphatidylcholine-specific phospholipase C, Drugs Exp. Clin. Res. 22 (1996) 287-294.

[15] M. Wu, M. Takemoto, H. Luo, J.J. Xu, M. H. Lu, M. Kameyama, T. Takumi, W.J. Song, A novel role of the antitumor agent tricyclodecan-9-yl-xanthogenate as an open channel blocker of KCNQ1/KCNE1, Eur. J. Pharmacol. 824 (2018) 99-107.

[16] R.M. Adibhatla, J.F. Hatcher, A. Gusain, Tricyclodecan-9-yl-xanthogenate (D609) mechanism of actions: a mini-review of literature. Neurochem. Res. 37 (2012) 671-679.

[17] K. Jynge, E. Dodson, Z. Derewenda, C. Little, L.K. Hansen, E. Hough, B. Birknes, S. Hansen, A. Hordvik, High-resolution (1.5 Å) crystal structure of phospholipase C from Bacillus cereus, Nature. 338 (1989) 357-360.

[18] S. Subramaniam, M. Mehrotra, D. Gupta, Virtual high throughput screening (vHTS) - A perspective, Bioinformation. 3 (2008) 14-17.

[19] R.V. Guido, G. Oliva, A.D. Andricopulo, Virtual screening and its integration with modern drug design technologies, Curr. Med. Chem. 15 (2008) 37-46.

[20] T. Zhu, S. Cao, P.C. Su, R. Patel, D. Shah, H.B. Chokshi, R. Szukala, M.E. Johnson, K.E. Hevener, Hit identification and optimization in virtual screening: practical recommendations based on a critical literature analysis, J. Med. Chem. 12 (2013) 6560-6572.

[21] T. Scior, A. Bender, G. Tresadern, J. Medina-Franco, K. Martínez-Mayorga, T. Langer, K. Cuanalo-Contreras, D.K. Agrafiotis, Recognizing Pitfalls in Virtual Screening: A Critical Review, J. Chem. Inf. Model. 52 (2012) 867-881.

[22] M.A. Clark, R.G.L. Shorr, J.S. Bomalaski, Antibodies prepared to Bacillus cereus phospholipase C crossreact with a phosphatidylcholine preferring phosoholipase C in mammalian cells, Biochem. Biophys. Res. Comm. 140 (1986) 114-119.

[23] L. Levine, D.M. Xiao, C. Little, Increased arachidonic acid metabolites from cells in culture after treatment with the phosphatidylcholine-hydrolyzing phospholipase C from Bacillus cereus, Prostaglandins. 34 (1987) 633-642.

[24] ChemBridge, DIVERSet™ Diverse Screening Libraries, (2018).

[25] C.A. Lipinski, F. Lombardo, B.W. Dominy, P.J. Feeney, Experimental and computational approaches to estimate solubility and permeability in drug discovery and development setting, Adv. Drug Deliv. Rev. 23 (1997) 3-25.

[26] S.F. Martin, P.J. Hergenrother, Catalytic cycle of the phosphatidylcholine-preferring phospholipase C from Bacillus cereus. Solvent viscosity, deuterium isotope effects, and proton inventory studies, Biochemistry. 38 (1999) 4403-4408.

[27] G. Jones, P. Willet, R.C. Glen, A.R. Leach, R. Taylor, Development and Validation of a Genetic Algorithm for Flexible Docking, J. Mol. Biol. 267 (1997) 727-748.

[28] M.D. Eldridge, C. Murray, T.R. Auton, G.V. Paolini, P.M. Mee, Empirical scoring functions: I. The development of a fast empirical scoring function to estimate the binding affinity of ligands in receptor complexes, J. Comp. Aid.Mol. Design. 11 (1997) 425-445.

[29] M.L. Verdonk, J.C. Cole, M.J. Hartshorn, C.W. Murray, R.D. Taylor, Improved protein-ligand docking using GOLD, Proteins. 52 (2003) 609-623.

[30] O. Korb, T. Stützle, T.E. Exner, Empirical Scoring Functions for Advanced Protein−Ligand Docking with PLANTS, J. Chem. Inf. Model. 49 (2009) 84-96.

[31] W.T.M. Mooij, M.L. Verdonk, General and targeted statistical potentials for protein–ligand interactions, Proteins. 61 (2005) 272-287.

[32] C.G. Bologa, T.I. Oprea, Compound collection preparation for virtual screening, Methods in molecular biology (Clifton, N.J.). 910 (2012) 125-143.

[33] A.P. Benfield, N.M. Goodey, L.T. Phillips, S.F. Martin, Structural studies examining the substrate specificity profiles of PC-PLC(Bc) protein variants, Arch. Biochem. Biophys. 460 (2007) 41-47.

[34] eMolecules, www.emolecules.com. (2018).

[35] ChemDiv, www.chemdiv.com, (2018).

[36] InterBioScreen, www.ibscreen.com, (2018).

[37] R.M. Coward, C.C. Carson, Tadalafil in the treatment of erectile dysfunction, Ther. Clin. Risk Man. 4 (2008) 1315-1329.

[38] R. Wang, S. Wang, How Does Consensus Scoring Work for Virtual Library Screening? An Idealized COmputer Experiment, J. Chem. Inf. Comput. Sci. 41 (2001) 1422-1426.

[39] J. Yang, Y. Chen, T. Shen, B.S. Kristal, D.F. Hsu, Consensus Scoring Criteria for Improving Enrichment in Virtual Screening, J. Chem. Info. Modeling. 45 (2005) 1134-1146.

[40] Y. Zhao, Auxin Biosynthesis: A Simple Two-Step Pathway Converts Tryptophan to Indole-3-Acetic Acid in Plants, Molecular Plant. 5 (2012) 334-338.

[41] S.Y. Kim, J.S. Ryu, H. Li, W. Park, H. Yun, K.J. Baek, N.S. Kwon, U.D. Sohn, D. Kim, UVB-activated indole-3-acetic acid induces apoptosis of PC-3 prostate cancer cells, Anticancer Res. 30 (2010) 4607-4612.

[42] Peter Wardman, Indole-3-Acetic Acids and Horseradish Peroxidase: A New Prodrug / Enzyme Combination for Targeted Cancer Therapy, Curr. Pharm. Design. 8 (2002) 1363-1347.

[43] S. Kim, D. Kim, S. Jeon, Y. Jeong, S. Kwon, K. Park, Hydrogen peroxide is a mediator of indole-3-acetic acid/horseradish peroxidase-induced apoptosis, FEBS Letters. 580 (2006) 1439-1446.

[44] D. Kim, S. Jeon, K. Park, Oxidation of indole-3-acetic acid by horseradish peroxidase induces apoptosis in G361 human melanoma cells, Cell. Signal. 16 (2004) 81-88.

[45] D.F. Veber, S.R. Johnson, H. Cheng, B.R. Smith, K.W. Ward, K.D. Kopple, Molecular Properties that Influence the Oral Bioavailability of Drug Candidates, J. Med. Chem. 45 (2002) 2615-2623.

[46] C. Eurtivong, J. Reynisson, The Development of a Weighted Index to Optimise Compound Libraries for High Throughput Screening, Mol. Inf. 38 (2019) e180006-n/a.

[47] H.M. Berman, J. Westbrook, Z. Feng, G. Gilliland, T.N. Bhat, H. Weissig, I.N. Shindyalov, P.E. Bourne, The Protein Data Bank, Nuc. Acids Res. 28 (2000) 235-242.

[48] Scigress: Version FJ 2.6 (EU 3.1.7), Fujitsu Limited 2008-2016.

[49] J. Reynisson, W. Court, C. O'Neill, J. Day, L. Patterson, E. McDonald, P. Workman, M. Katan, S.A. Eccles, The identification of novel PLC-c inhibitors using virtual high throughput screening, Bioorg. Med. Chem. 17 (2009) 3169-3176.

[50] E. Robinson, E. Leung, A.M. Matuszek, N. Krogsgaard-Larsen, D.P. Furkert, M.A. Brimble, A. Richardson, J. Reynisson, Virtual screening for novel Atg5–Atg16 complex inhibitors for autophagy modulation, Med. Chem. Comm. 6 (2015) 239-246.

[51] T. Khomenko, A. Zakharenko, T. Odarchenko, H.J. Arabshahi, V. Sannikova, O. Zakharova, D. Korchagina, J. Reynisson, K. Volcho, N. Salakhutdinov, O. Lavrik, New inhibitors of tyrosyl-DNA phosphodiesterase I (Tdp 1) combining 7-hydroxycoumarin and monoterpenoid moieties, Bioorg. Med. Chem. 24 (2016) 5573–5581.

[52] R. Huang, D. Ayine-Tora, M.N.M. Rosdi, Y. Li, J. Reynisson, I.K.H. Leung, Virtual screening and biophysical studies lead to HSP90 inhibitors, Bioorg. Med. Chem. Lett. 27 (2017) 277-281.

[53] A.R. Leach, V.J. Gillet, 1. Representation and manipulation of 2D molecular structures, An Introduction to Chemoinformatics. (2003) 1-26.

[54] R. Todeschini, M. Lasagni, E. Marengo, New molecular descriptors for 2D and 3D structures. Theory, J. Chemometrics, 8 (1994) 263-272.

[55] C.A. Tan, M.J. Hehir, M.F. Roberts, Cloning, Overexpression, Refolding, and Purification of the Nonspecific Phospholipase C from Bacillus cereus, Protein Expres. Pur. 10 (1997) 365-372.

[56] P. Ravasi, M. Braia, F. Eberhardt, C. Elena, S. Cerminati, S. Peirú, M.E. Castelli, H.G. Menzella, High-level production of Bacillus cereus phospholipase C in Corynebacterium glutamicum, J. Biotech. 216 (2015) 142-148.

Highlights

Virtual screen resulted in inhibitors for Phosphatidylcholine–specific phospholipase C

Pyrido[3,4-*b*]indoles and morpholinobenzoic acid drug-like series identified

Single digit micro-molar potency reached

Declaration of interests

☒ The authors declare that they have no known competing financial interests or personal relationships that could have appeared to influence the work reported in this paper.

☒The authors declare the following financial interests/personal relationships which may be considered as potential competing interests:

On behalf of all the authors

Jóhannes Reynisson
11/11 2019